J. L. MUÑOZ*, G. ROJO*, I. UNAMUNO*, J. J. LARAUDOGOITIA*

ANALYSIS OF AC EAF ELECTRICAL MAGNITUDES FOR DIFFERENT PROCESS CONDITIONS USING A MODIFIED CIRCULAR DIAGRAM PERSPECTIVE

ANALIZA WIELKOŚCI ELEKTRYCZNYCH PIECA ŁUKOWEGO PRĄDU ZMIENNEGO DLA RÓŻNYCH WARUNKÓW PROCESU Z UŻYCIEM WYKRESU KOŁOWEGO

In this work power data measured in an AC electric arc furnace is analysed. It is observed that the distribution of measured values, when plotted in an active vs. reactive power diagram (circular diagram), don't lie on a standard circular diagram curve of constant voltage, but rather lie on a curve of constant apparent power. This is associated with the time span of the data collected that is much greater (minutes) than the used in theoretical analysis of EAF electrical variables. In this time scale the electrode regulation system effect dominates.

Using the apparent power diagrams and the considerations that justify them, several phenomena observed at Sidenor Basauri works EAF are explained.

Keywords: Electric Arc Furnace, electrode regulation, active power, reactive power, circular diagram, slag foaming

W tym artykule poddano analizie dane ze zmierzonej mocy w elektrycznym piecu łukowym prądu zmiennego. Zauważono, że rozkład zmierzonych wartości umieszczonych na wykresie mocy czynnej, w zależności od mocy biernej (wykres kołowy), nie leży na standardowej krzywej stałego napięcia, a raczej na krzywej stałej mocy pozornej. Łączy się to z czasem zbierania danych, który jest znacznie dłuższy niż użyty do teoretycznej analizy zmiennych elektrycznych pieca łukowego. W tej skali czasu dominował efekt systemu regulacji elektrodami.

Używając wykresów mocy pozornej i założeń, które to uzasadniają, zostało wyjaśnionych kilka zjawisk zaobserwowanych w pracy pieca łukowego w stalowni Sidenor Basauri.

1. Introduction

In order to optimize the electrical behaviour of a high power AC EAF it is essential to use reliable data description tools. This is not a task as simple as could be thought due to the complexity of the system that results in variability and fluctuations of variables and depends even on how the electrical magnitudes are measured or obtained. A usual way of describe an electrical system is using the so-called circular (or PQ) diagram, where active power P is plotted versus reactive power Q. In this diagram the working points corresponding to a certain secondary voltage are located along a semi-circular shaped curve (that can be deformed if a variable operational reactance is considered). An example of a typical circular diagram is shown in Fig. 1.

The ideal circular diagram is a useful design tool. It is obtained from equations Eq. 1, where U is the tension, X is the short-circuit reactance and $cos\phi$ is the power factor. For a given secondary tension selected by the chosen transformer tap, and assuming a constant reactance Eq. 1 represents the parametric equations of a circumference. Using this diagram it is possible to define the right set points of operation in order to achieve the highest active power within the arc stability limits.

$$\begin{cases} P = \frac{U^2}{X} \sin\varphi \cos\varphi \\ Q = \frac{U^2}{X} \sin^2\varphi \end{cases} \qquad (1)$$

During EAF operation, the circuit reactance is higher than the short-circuit reactance, mainly due to the non-linearity of the electric arc resistance. This operating reactance is higher than the short-circuit one, and several theoretical models can be found to explain or describe its value [2-4]. The modified circular diagram curve can also be computed using expressions fitted from measured

* SIDENOR I+D S.A., BARRIO UGARTE S/N, 48970 BASAURI (SPAIN)

operational data, for example, numerically solving the coupled equations in Eq 2, where constants *a* and *b* are obtained from a linear regression of measured reactance and intensity. An example of modified curve is shown in Fig. 1.

$$\begin{cases} I = \frac{U}{S} \sin \varphi \\ X = a + \frac{b}{I^2} \end{cases} \qquad (2)$$
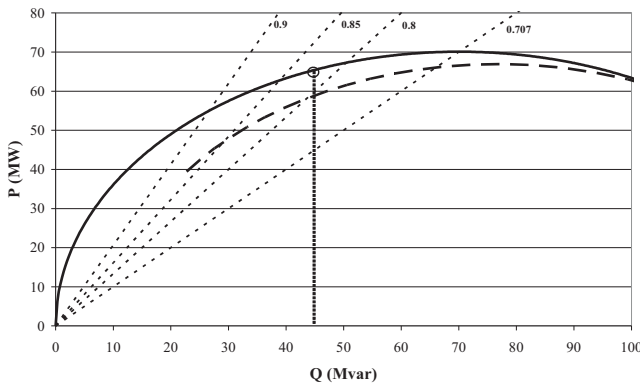

Fig. 1. An example theoretical circular diagram, showing the working curve for a constant operating reactance (solid line) and the corresponding to an intensity dependent reactance (dashed line). The locus of constant power factor (dashed lines) is also drawn for different power factor values, along with a selected working point

The theoretical working curve drawn on a PQ diagram describes the physical phenomena happening when the electric arc is considered as an element of the electric circuit of the EAF. More complex theoretical descriptions of the three-phase system can also be found in literature [5, 6]. However, when plotting real operational data obtained from electrical magnitudes measured during furnace operation in such a diagram the interpretation of the result is not straightforward, and it even depends on how the magnitudes are measured or derived from other measured quantities.

In this work the values of active and reactive power are analyzed by means of plotting them in a circular diagram. The distribution of experimental data for a given operational condition (transformer tap, intensity set point) measured during a long time span for a heat (several minutes) cannot be described using the theoretical equations that govern the evolution for short times (one or two cycles of the AC system). In order to extract information about the process from these PQ graphs, another cause must be considered: the electrode regulation systems, which is the modulator of the distribution of experimental points in the graph. So, in order to use the familiar and easy to draw circular diagram, some considerations on how the electrode regulation system modifies the working points in the diagram must be done. This is the subject of the present paper.

2. Characteristics of the EAF under study

The EAF that has been analysed is located at Sidenor Basauri Works. SIDENOR INDUSTRIAL S.L. is a steelmaking company producing special and stainless steel long products, devoted to a high extent for automotive applications. Production facilities at Sidenor Basauri plant include electric arc furnace, secondary metallurgy station (two ladle furnaces sharing a vacuum degasser tank and VOD) and continuous casting process followed by direct rolling.

The EAF is an AC SMS-DEMAG furnace with a capacity of 150 tons of liquid steel. Furnace is powered by a 150 MVA Tamini transformer, with 18 secondary taps ranging from 650 V to 1300 V (for a primary voltage of 30 kV). Connection is triangle-triangle. Series reactor with off-load tap changer (with on-load bypass system) is installed with 5 taps (from 0 to 1.20 Ω). Filters for 2nd, 3rd and 4th harmonic are also installed. Short-circuit resistance and reactance are 0.41 mΩ and 4.55 mΩ, respectively. The electrode regulation system in operation when the data was collected for this work was made by Electrotechnology.

In the standard process for a SBQ heat, scrap is loaded in two baskets of about 80 and 60 tons. During scrap meltdown active powers around 87 MW are achieved, using long arcs and high secondary voltage. The slag foaming practice starts at about 35000 kWh, after the second basket has been melted, and the average active power during this stage of the process is near 85 MW. Electrode regulation works with a constant intensity setup. Primary and secondary voltage and current and active power are measured and stored in a process database (Oracle) for offline analysis, where data is recorded with a two seconds rate. Power profile and intensities for a typical heat are depicted in Fig. 2.

When slag foaming starts an automatic oxygen and graphite injection system controls the process in order to assure good quality foam and to reach the right level of oxygen activity at taping, that can range from 200 to 800 ppm depending on the steel grade produced. This is done by monitoring acoustic noise and harmonic distortion, along with temperature and oxygen activity measurements. This automatic control assures a good quality of the foaming with very stable electrical behaviour. Variations in active power during the process are related to the response of the automatic injection system, that changes slag conditions during the process.
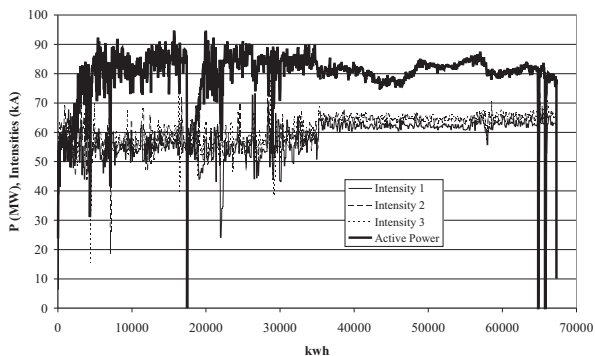
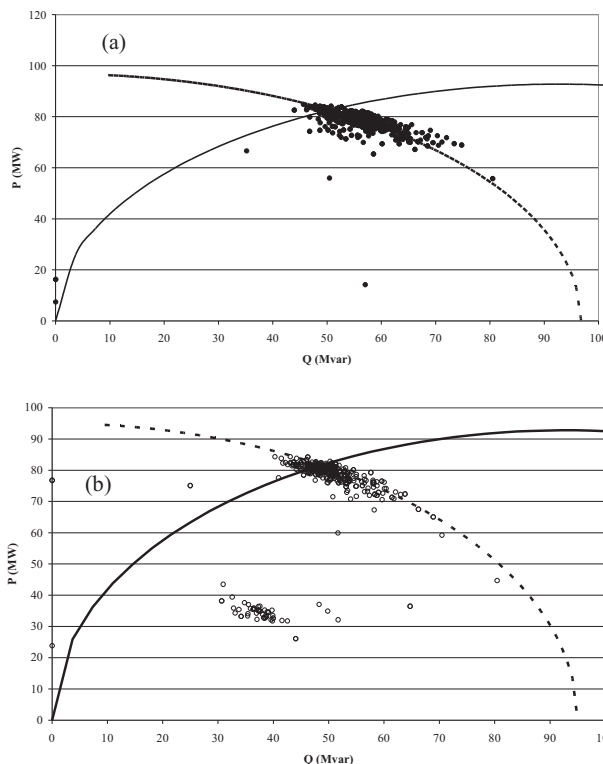Fig. 2. Intensity and active power for a typical heat

Fig. 3. Active and reactive power measured data during slag foaming (a) and melting (b) for a heat. Solid curve corresponds to the theoretical circular diagram of constant voltage, whereas dashed line corresponds to a curve of constant apparent power

3. Active and reactive power measurements interpretation

Active power is directly measured by the data acquisition system. Reactive power is obtained from apparent power using Eq. 3. This method of obtaining the apparent power S from rms values of intensities and tensions is preferred over computing it from active power and a measured power factor.

$$S = \sum I_i V_i$$
$$Q = \sqrt{S^2 - P^2}. \tag{3}$$

Data measured in this way is shown in fig. 3. Each point in the graphs corresponds to an average for two seconds. In fig. 3a the data is taken during slag foaming stage of the process, and all the points correspond to the same operational conditions (transformer tap and intensity set point). It is clear that the distribution of working points don't match the standard circular diagram curve (a curve of constant voltage) but seem to fit a constant apparent power curve (a constant S curve). The same is shown in fig. 3b for data taken during the melting stage of a heat.

The distribution of measured points along the constant-S curve may be a consequence of how data is processed (P is directly measured and Q is derived using Eq. 3) and averaged (each point is the rms average for two seconds), and can be also related to some particularity of the EAF under study. Nonetheless, this result has been observed in a consistent way for a good number of heats, even when measurements are performed by independent analysts using different equipment. Independently of the theoretical justification of the cloud of points shape we are interested in extract information about the process from these graphs, so they have been used in the analysis of the furnace for different process conditions.

In our interpretation we conclude that the observed behaviour is a consequence of the electrode regulation system, whose effects are noticeable in the time scale (several seconds) that is being considered in the measurements. In a short time scale (a cycle) the characteristics that determine the arc behaviour (voltage, reactance, arc length) can be considered stable, and the relationships among them can be obtained theoretically or from experimental measurements of wave forms, and expressions relating operational reactance to intensities (like Eq. 2) can be obtained. But in a longer time scale these relationships are no longer valid, because they are superseded by a stronger (but slower) driving force, that is, the electrode regulation system.

As the electrical magnitudes change continuously during process in order to keep a selected working point (for example a constant intensity), an active system that is able to dynamically change some parameter is required. This is the task of the regulation system, that monitors some system variable (intensities, impedance, power ...) and moves electrodes up or down until the right value is achieved. The movement of the electrodes, that is the response of the regulation system, is much slower than the fluctuations that are taking place in the arcs. So when we look at the system in a long time scale

the observed results are controlled by the regulation, and not by other short time effects.

In the long scale (several minutes) that is our focus of interest in this work, if operational settings (tap, intensity) are not changed the secondary intensity is constant. Intensity will fluctuate a lot and it can't be considered constant in a short time scale, but in the long scale regulation dominates, so on average intensity can be taken as constant. Thus, the fluctuations in the arc behaviour in the long scale cannot manifest as intensity variations, because it is kept constant by the regulation, so it manifests as variations in tension and power factor. But using the same argument in the long scale tension is also constant (transformer tap) so the only degree of freedom is the power factor.

Once the working point is chosen (a point in the PQ diagram) the fluctuation of the measured points during a several minutes span of time will not distribute along the constant-V curve in the diagram, but in a curve in which VI is constant, that is, a curve of constant apparent power, S.

This phenomenological description is valid for our purpose, that is, to explain phenomena that take place in a steelmaking plant using data easy to obtain and considering simple laws. For more in depth analysis of experimental data the theoretical models of arc wave forms, operational reactance and equivalent circuits are needed, but for the description of everyday, macroscopic events a simplified view can be helpful. Let's see some applications of this.

4. Applications

Response to an increase of primary voltage

Due to maintenance operations in the substation yard at Sidenor Basauri plant, the second harmonic filter was down during some time. When it was working again, an increase in the primary voltage of the EAF transformer from 30.5 kV to 32.0 kV was observed, as it was expected.

Comparing power data before and after the primary voltage increase and separating data collected during main melting phase and during slag foaming, different behaviour is observed. For data collected from slag foaming stage the averaged reactive power remains constant after the change, while the apparent power is higher (fig. 4). This is not observed for data collected during main melting phase, where reactive power and apparent power both increase (fig. 5). Active power logically increases in both cases. This different behaviour can be explained using the constant apparent power diagram.
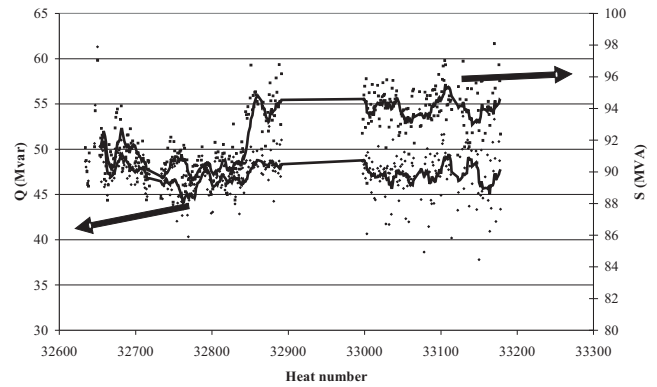

Fig. 4. Averaged reactive and apparent power for a sequence of heats, measured during slag foaming stage. Different behaviour after a primary voltage increase happens is observed
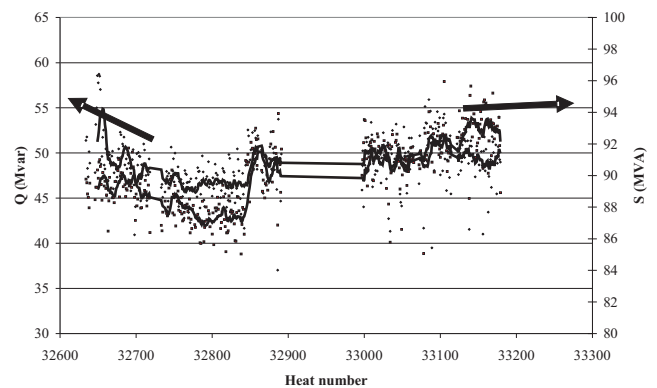

Fig. 5. Averaged reactive and apparent power for a sequence of heats, measured during main melting stage of each heat

The higher voltage is translated into a longer arc length. The reactive power during slag foaming has the same value before and after the change because, first, secondary intensity is the same (due to the electrode regulation set point) and, second, because operating reactance has the same value: the minimum possible value. Slag foaming stabilises the arc in such way that despite of the arc length the measured reactance is approximately the short-circuit reactance. We are supposing the in both situations the arc is fully covered by the foamy slag. So reactive power, that can be expressed as

$$Q = 3XI^2 \tag{4}$$

remains constant. On the other hand, apparent power logically increases because voltage is higher and intensity is constant. In a circular diagram, the new average working point obtained after the primary voltage increase is obtained by a vertical displacement from the point P1 (that lies on the S1 curve) to P2 (that lies on the S2 curve) as it is depicted in fig. 6. As active power increases while reactive power doesn't, power factor must also increase. This is confirmed by the data collect-

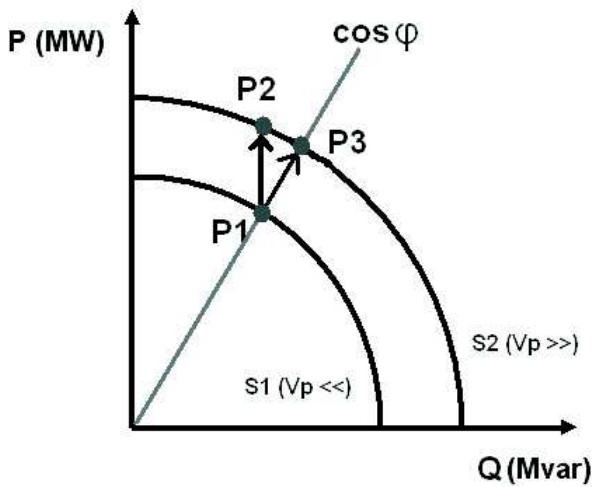ed: average power factor (computed as *P/S*) raises from 0.855 to 0.864 with the primary voltage increase.

Fig. 6. Schematic circular diagram showing two constant apparent power curves (S1 and S2) and the transition of a working point from S1 to S2 depending if it corresponds to melting or slag foaming stages of the process

For the data collected during main melting phase the increase in primary voltage results in increases both of apparent and reactive power (along with active power). As before, the higher primary voltage is converted into a higher secondary voltage, while intensity is the same due to the regulation set point, that has elevated the electrodes to a higher position in order to get a longer arc with higher resistance to obtain the same intensity with higher voltage. On opposition to the slag foaming situation an increase of arc length results in less stable arcs with a higher reactance. So although intensity is the same reactive power increases due to the higher operating reactance.

In the circular diagram, the operating point after the change in primary voltage will move from a point in the constant-S S1 curve to a point in the S2 curve with higher *Q* and *P*. As both powers change more or less in the same way, the translation from one point to the other is done along a line of constant power factor, so the new point can be computed as the cross of the line that contains P1 and the origin and the S2 curve. The equal power factor before and after the voltage increase is also confirmed experimentally, as the average values of power factor *P/S* are equal to 0.84 in both situations.

Slag foaming quality and active power

A similar effect to the previously described appears also in a different context. A foamy slag quality assessment technique is used at Sidenor Basauri plant, as it is described elsewhere [7, 8]. If the slag foaming process is correctly done, a low noise index is obtained, measured both using acoustic noise and electric THD (Total Harmonic Distortion). If for some reason a good foaming is not achieved (for example due to problems in oxygen or graphite injection) then a high noise index is obtained.

Relating the slag foaming noise index with the electrical variables (active power and secondary voltages) measured in the furnace during the process an interesting result is observed. When the noise index is low, meaning that a very good foaming has been reached a strong correlation between measured active power and averaged secondary voltage is observed. But if noise index is high, this dependence is not observed and both variables are uncorrelated.

The described behaviour can be explained using the same arguments than for the higher primary voltage situation. In the case of having a low noise index, with good quality foam, the slag covers the arcs completely, so the operating reactance will be the lowest possible value (close or equal to the short-circuit reactance), regardless of arc length and secondary voltage. As secondary intensity is the same in all the process (due to the regulation and in the long time scale), arc length is directly proportional to voltage, and so is arc resistance. This results in an active power proportional to secondary voltage through

$$P = 3RI^2 = S \cos \varphi \qquad (5)$$

while reactive power remains constant. Voltage fluctuations during slag foaming process results in directly related active power fluctuations (for low noise index). This can be written as:

$$\frac{dP}{dV} = S \frac{d(\cos \varphi)}{dV} \approx const. \qquad (6)$$

On the contrary, if the foaming achieved is not good enough (for example as result of oxygen or graphite injection malfunction or non standard slag composition) the noise index will be high. In this situation the variation in arc length caused by a variation in secondary voltage will result in a variation of both resistance and reactance, so the voltage fluctuations don't result in power factor fluctuations. It can be said that, approximately, reactance and resistance both changes in the same way so power factor is the same. In this situation Eq. 6 must be changed to

$$\frac{dP}{dV} = S \frac{d(\cos \varphi)}{dV} \approx 0 \qquad (7)$$

This explains why the active power and the averaged secondary voltages are not correlated when a high noise index is detected.

5. Conclusions

In this work power data coming from an AC EAF has been analysed using a PQ diagram. It is observed that for a given operation set points (secondary voltage and intensity) the distribution of active and reactive power points in the diagram lies on a curve of constant apparent power (S) rather than in a constant voltage curve, as it is used for theoretical determination of set points. This is explained considering the long time scale of the measurements, where the constant intensity electrode regulation system response dominates over other effects.

Making use of the interpretation of the diagram as a constant-S diagram, we have explained several phenomena observed in the EAF under study. The increase of primary voltage resulted in a higher apparent power, but for data collected during foamy slag this is not translated in higher reactive power, that remained the same. This is not observed for data coming from main melting stage, where apparent and reactive power both increase. Also, the different relationship observed between active power and secondary voltage during slag foaming when the noise index is high or low is also explained.

Acknowledgements

REFERENCES

[1] M. K. F. K n o o p, S. K ö h l e, Electrical design of high voltage, high reactance a-c arc furnaces, Iron and Steel Engineer **24**, p. 243 (2004).

[2] S. K ö h l e, Lineares eleltrishes Ersatschaltbild von Drehstrom-Lichtbogenöfe. Bericht Nr.2.2.14, 10. UIE-Kongress, Stockholm (1984).

[3] S. K ö h l e, M. K n o o p, R. L i c h t e r b e c k, Lichbogenreaktanzen von Drehstrom-Lichtbogenofen. Elektrowärme international **51**, B4, (175-185) (1993).

[4] B. B o w m a n, Computer modelling of arc furnace electrical operation, Metallurgia International **1**, (286-291) (1988).

[5] B. B o w m a n, Solution of arc-furnace electric circuit in terms of arc voltage, Ironmaking Steelmaking, 4, 178 (1982).

[6] A. W a s o w s k i, Modified solution of arc furnace electrical circuit in terms of arc voltage, Ironmaking Steelmaking, **18**, 5, 354 (1991).

[7] B. K l e i m t, J. C. B a u m e r t, S. L a n d a, R. K ü h n, Dynamic control of EAF burners and injectors for carbon and oxygen for improved and reproducible furnace operation and slag foaming, RFCS Steel RTD Programm, Contract RFS-CR-03031 (2007).

[8] S. L a n d a, T. R o d r i g u e z, J. L. M u ñ o z, J. J. L a r a u d o g o i t i a, Dynamic control of slag foaming at Sidenor Basauri meltshop. Proceedings of the 9EES Conference.